



CHALMERS
UNIVERSITY OF TECHNOLOGY

GaN HEMT with superconducting Nb gates for low noise cryogenic applications

Downloaded from: <https://research.chalmers.se>, 2024-04-28 15:19 UTC

Citation for the original published paper (version of record):

Mebarki, M., Ferrand-Drake Del Castillo, R., Pavolotskiy, A. et al (2022). GaN HEMT with superconducting Nb gates for low noise cryogenic applications. 2022 Compound Semiconductor Week, CSW 2022. <http://dx.doi.org/10.1109/CSW55288.2022.9930458>

N.B. When citing this work, cite the original published paper.

GaN HEMT with superconducting Nb gates for low noise cryogenic applications

Mohamed Aniss Mebarki^{1*}, Ragnar Ferrand-Drake Del Castillo², Alexey Pavolotskiy¹, Denis Meledin¹, Erik Sundin¹, Mattias Thorsell², Niklas Rorsman², Victor Belitsky¹, Vincent Desmaris¹

¹: Group for Advanced Receiver Development, Chalmers University of Technology, Gothenburg, Sweden

²: Microwave Electronics Laboratory, Chalmers University of Technology, Gothenburg, Sweden

Email: aniss@chalmers.se

Abstract—We report on the successful integration of superconducting Nb gate electrodes to AlGaIn/GaN heterostructures and HEMTs for low noise cryogenic applications. First, a specific Nb-gate process was developed and implemented on stand-alone gate test structures. The latter were tested at cryogenic temperatures down to 4 K, using DC end-to-end measurements. The results show a clear transition to a superconducting state at $T_c \sim 9.2$ K. The superconducting nature of the Nb gates further verified on actual HEMTs, featuring 2 fingers design with gate length of $0.2 \mu\text{m}$, through their S-parameters measurements at $T < T_c$. Finally, we demonstrate a significant reduction of the gate resistance with superconducting Nb compared to Au-gated transistor with the identical dimensions. The results confirm the potential of the GaN HEMTs with superconducting Nb-gate for low noise operation at cryogenic temperatures.

Keywords—GaN; Nb; cryogenic HEMT

I. INTRODUCTION

In addition to excellent power performances, High Electron Mobility Transistors (HEMT) based on Gallium Nitride (GaN) may also find applications in reliable low noise amplifiers (LNA). On the basis of the recent reports on the improvement of its noise performances at low temperatures [1], this technology emerges as a novel candidate for the low noise cryogenic applications in deep space communication, radio astronomy and quantum computing. For a successful integration, an ultimate reduction of the noise temperature of GaN HEMTs is required. Due to the dominant thermal origin of the noise at high frequencies, the resistances of the metallic electrodes are one of the devices' noise main contributors. In particular, the gate resistance, denoted R_g , is significantly affecting both the HEMT's noise and RF performances. One way to address this challenge could be to rely on the properties of the superconducting materials, in which the resistance tends to zero below a critical temperature T_c . In this perspective, we explore and successfully demonstrate the possibility of using GaN HEMTs with superconducting Nb gate.

II. Results and discussion:

The present study is based on AlGaIn/GaN on SiC HEMTs fabricated in-house, presenting a typical Hall mobility of $2090 \text{ cm}^2/\text{V} \cdot \text{s}$ and a sheet charge density of $1.09 \times 10^{13} \text{ cm}^{-2}$ at room temperature (RT). The process details are described in [2], with an epi-design employing Fe-doped buffer. The Nb gates were deposited by means of dc magnetron sputtering. The Nb thickness was set to $0.3 \mu\text{m}$, corresponding to more than 3 times its London penetration depth, to minimize RF losses. This parameter defines the main advantage of the superconducting Nb over the other normal metals, which is the absence of conduction losses independently of the frequency of operation in the microwave range [3]. The technological process was developed taking particular attention to prevent the formation of superconducting weak links at the mesa edge. Au-gated devices were included in the same die for comparisons.

The evaluation of the critical temperature of the superconducting Nb-gates for various geometrical dimensions was performed. For this purpose, 1-finger test structures were specifically designed and fabricated. Their end-to-end gate resistance, R_{g-ee} , was measured using 4-points measurements, as illustrated in Fig. 1a. Fig. 1b shows a microscopic image of a typical test structure. Several gate lengths, L_g , and gate widths, W_g , of these structures were tested in order to study the scaling properties of the superconducting electrode. The measured R_{g-ee} versus temperature down to 4 K is shown in figures 2a and 2b. A superconducting transition is clearly observed at $T_c \sim 9.2$ K. Simultaneously, these results demonstrate the successful integration of the superconducting Nb to the GaN-based heterostructures: the gate presents an absolute zero DC resistance for $T < T_c$. We note, however, a shift of T_c towards lower temperatures for reduced gate lengths which possibly indicates that the gate dimensions and topology may locally affect the Nb properties.

Furthermore, 2-fingers HEMT devices of $L_g = 0.2 \mu\text{m}$ and a total gate width of $25 \mu\text{m}$ were measured in a cryogenic probe station. SEM picture of the device is shown in Fig. 1c. The Au-gated device with the identical dimensions was also measured at both RT and the cryogenic temperature. Both devices presented similar excellent DC characteristics, shown in Fig. 3 and Fig. 4, which significantly improved when cooled down. R_g was then extracted from the S-parameters using the approach in [4], with $V_{DS} = 0 \text{ V}$. The results are reported in Fig. 5 and Fig. 6. At RT, the extracted small-signal gate resistance, R_{g-Nb} , is approximately twice higher than R_{g-Au} . However, at temperature below T_c , R_{g-Nb} drops by a factor of 16 at $V_{GS} = 0 \text{ V}$ compared to RT, while this ratio is only 4.4 in the case of R_{g-Au} . The R_{g-Nb} becomes then distinctly lower than R_{g-Au} for $T < T_c$.

These results show the possible advantage of using GaN HEMTs with superconducting-Nb gate over the conventional Au-gates. In fact, given the superconducting nature of the Nb gates, the gate resistance is considerably reduced. Further measurements and analysis are conducted in order to determine the critical drain current and the impact on the low noise amplifiers design perspectives.

References :

1. V. Desmaris et al., ISSTT 2019 - 30th International Symposium on Space Terahertz Technology, 67-68, (2019)
2. D.-Y. Chen et al, IEEE Electron Device Letters, 41.6, 828-831, (2020)
3. V. Belitsky et al., 2007 Int. J. Infrared Millimeter Waves 27-809 (2009)
4. N. Rorsman et al. IEEE Transactions on Microwave Theory and Techniques 44.3,432-437, (1996)

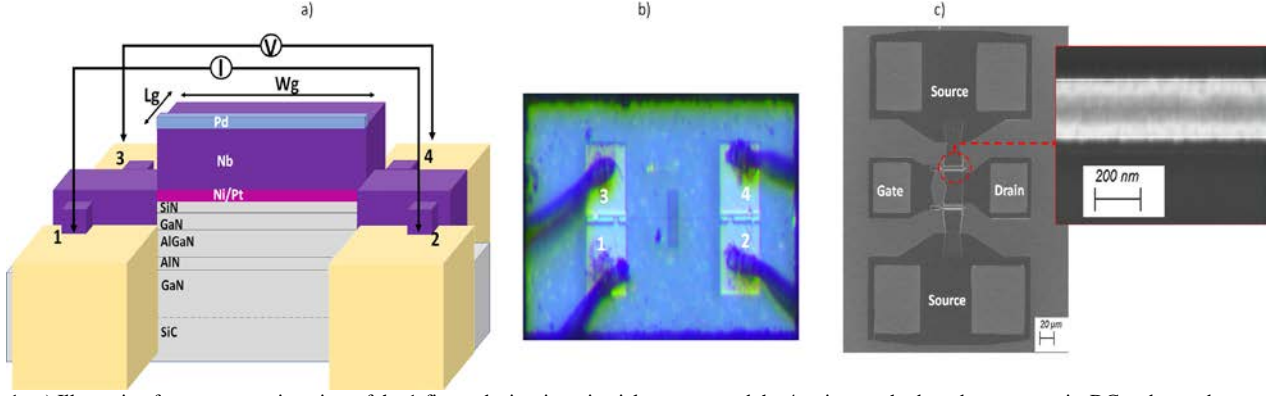


Fig. 1. a) Illustration from cross section view of the 1-finger device, its epitaxial structure and the 4-points method used to measure its DC end-to-end gate resistance. From the gate finger, a pair of electrodes is used to drive a current while the voltage drop is collected via another pair. b) Microscopic image of the 1-finger device with bond wires. c) SEM image of the 2x25 μm device (left), zoom on its 0.2 μm long gate finger (right).

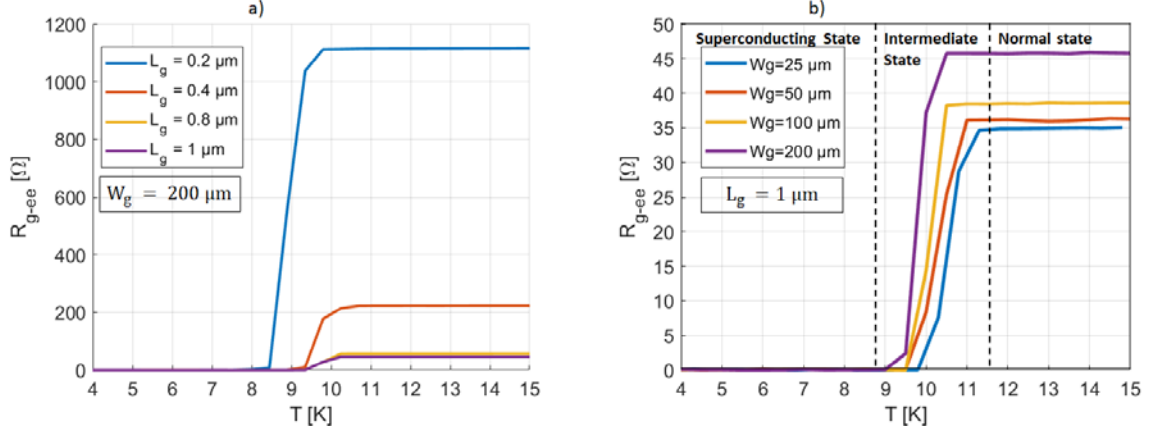


Fig. 2. Results of the DC end-to-end gate resistance measurements from the 1-finger devices a) Variation of $R_g(T)$ for different L_g and $W_g = 200 \mu\text{m}$. b) $R_g(T)$ for different W_g and $L_g = 1 \mu\text{m}$.

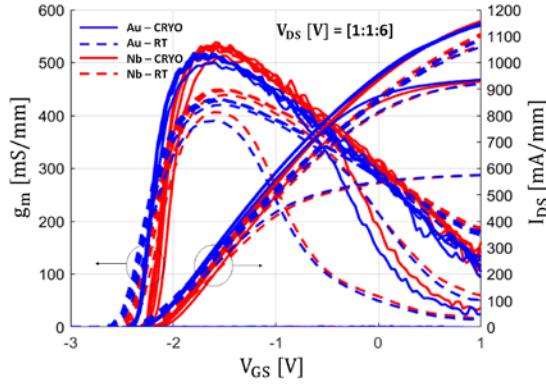


Fig. 3. $I_{DS}(V_{GS})$ and $g_m(V_{GS})$ characteristics of the 2x25 μm with $L_g = 0.2 \mu\text{m}$ with Nb-gate (red) and Au-gate (blue) at RT (dashed lines) and $T < T_c$ (continuous line).

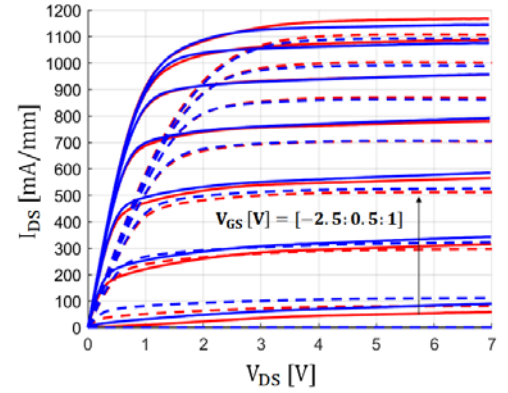


Fig. 4. $I_{DS}(V_{DS})$ characteristic of the 2x25 μm with $L_g = 0.2 \mu\text{m}$ with Nb-gate (red) and Au-gate (blue) at RT (dashed lines) and $T < T_c$ (continuous line).

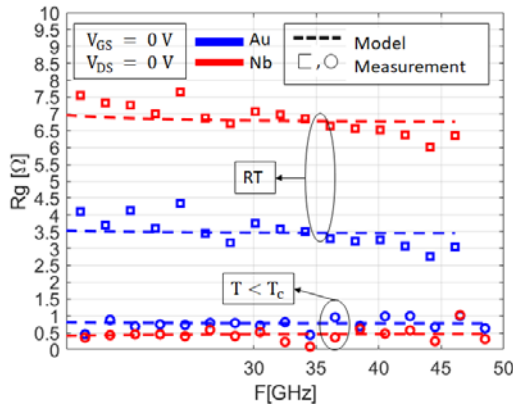


Fig. 5. Comparisons of the measured Z-parameters at RT and $T < T_c$ with the frequency-dependent model used to extract R_g , for $V_{GS} = V_{DS} = 0 \text{ V}$, from 2x25 μm device with $L_g = 0.2 \mu\text{m}$. R_g is obtained from the real part of $(Z_{11} - Z_{12})$ at high frequencies.

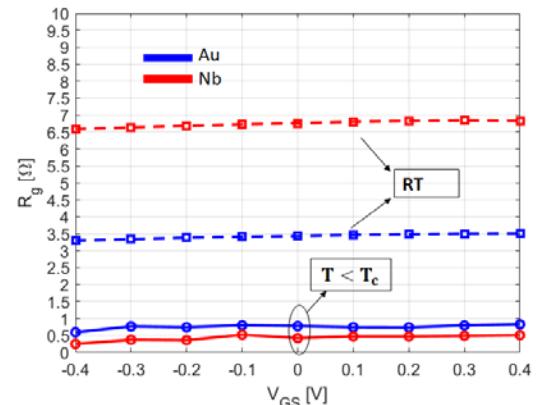


Fig. 6. The V_{GS} -dependence of R_{g-Au} and R_{g-Nb} , under $V_{DS} = 0 \text{ V}$, as extracted from the S-parameters measurements at RT and $T < T_c$ from 2x25 μm device with $L_g = 0.2 \mu\text{m}$